Arctic Climate

MC Serreze, University of Colorado, Boulder, CO, USA

Synopsis

Key features of the Arctic, such as its low mean annual air temperature, stable boundary layer, sea ice cover, permafrost, and snow cover, largely result from limited solar radiation receipts as compared to lower latitudes. The high albedo of snow and ice helps to maintain the Arctic in a low thermal energy state. However, regional features of the atmospheric and ocean circulation and surface modify primary latitudinal controls to result in a variety of climate conditions across the Arctic. Recent decades have seen pronounced changes in the Arctic, including reductions in sea ice extent, largest in September, and rises in surface air temperature, largest in autumn and winter.

Physical Features of the Arctic

The Arctic is defined as the region lying north of the Arctic Circle (66.5622° N latitude). In the north of the Arctic Circle, the sun remains above the horizon for 24 h (polar day) at least 1 day per year and below the horizon for 24 h (polar night) at least 1 day per year. On the Arctic Circle those events occur at the June and December solstices, respectively. The North Pole (90° N) experiences 6 months of polar day and 6 months of polar night.

Most of the region north of 70° N is occupied by the Arctic Ocean. Except for the sector straddling the date line between about 20° E and 20° W, the ocean is surrounded by land. Because of its largely landlocked nature, the Arctic Ocean is sometimes referred to as a Mediterranean-type sea. The dominant feature of the ocean surface is its floating sea ice cover. Northern Hemisphere sea ice extent, defined as all areas with an ice concentration (a fractional ice coverage) of at least 15%, waxes and wanes with the seasons (Figure 1(a) and 1(b)), typically ranging from upward of 15×10^6 km^2 in March to 7×10^6 km^2 or lower in September. These figures include seasonal ice in areas such as the Sea of Okhotsk, the Bering Sea, and Hudson Bay Ice that lie south of the Arctic Circle. The ice cover can be divided into first-year ice that is formed in a single ice growth season, and multiyear ice, which is ice that has survived one or more summer melt seasons. Any first-year ice present at the end of the melt season in September hence gets promoted to multiyear ice. Sea ice thickness ranges widely from a thin veneer to locally over 10 m. The probability distribution of sea ice thickness has a peak of about 3 m. While multiyear ice tends to be thicker than first-year ice, ridging and rafting can result in very thick first-year ice. Because of brine rejection during its formation, sea ice is nearly freshwater. For ice thicker than 1 m, a salinity of 2–6 parts per thousand is typical. Due to subsequent brine drainage by gravity, salinities for multiyear ice are considerably lower.

Apart from areas of land fast ice, the sea ice cover is in near-constant motion. The large-scale mean annual drift pattern is characterized by the clockwise Beaufort Gyre, centered over the Beaufort Sea north of Alaska, and the Transpolar Drift Stream, a motion of ice from the Siberian coast, across the pole and through Fram Strait (the strait at about 80° N separating Greenland from the Svalbard Archipelago) (Figure 2). This pattern reflects roughly equal contributions by winds and surface ocean currents, the latter ultimately wind driven to a large extent. The mean annual sea ice circulation hence broadly resembles the mean annual sea level circulation of the atmosphere. Mean annual drift speed ranges from 1 to 5 cm s^{-1} in the Beaufort Gyre and tends to increase along the Transpolar Drift Stream and through Fram Strait, where mean values may exceed 10 cm s^{-1}.

Snow cover atop the sea ice cover of the central Arctic Ocean is generally present for 10 months of the year. Most of the surrounding land surface of the Arctic is snow covered from October through May, with the duration of snow cover increasing with latitude. However, precipitation is generally scant in the Arctic. Some of the land, such as in the Canadian Arctic Archipelago, is classified as polar desert, often with less than 5% plant cover. In lower Arctic latitudes, the tundra commonly includes shrub vegetation of birch and willow. Permanent land ice is primarily restricted to the Greenland ice sheet (containing about 7 m of global sea level equivalent) and the ice caps and glaciers of the northeastern Canadian Arctic Archipelago, and the archipelagos of Svalbard, Novaya Zemlya, Severnaya Zemlya, and Franz-Josef Land. However, most Arctic land is underlain by perennially frozen ground (permafrost), overlain by an active layer exhibiting seasonal thaw. Permafrost acts as an impermeable barrier. As a result, many areas are covered by shallow thaw lakes in summer.

Atmospheric Circulation

Large-Scale Features

The primary feature of the northern high-latitude mid-tropospheric circulation is the polar vortex. The vortex is strongly asymmetric during winter (Figure 3(a)) with major troughs over eastern North America and eastern Eurasia and a weaker trough over western Eurasia (the Urals trough). A strong ridge is located over western North America. The lowest tropospheric pressure heights in winter are located over northern Canada. These features are related to orography, land–ocean distribution, and

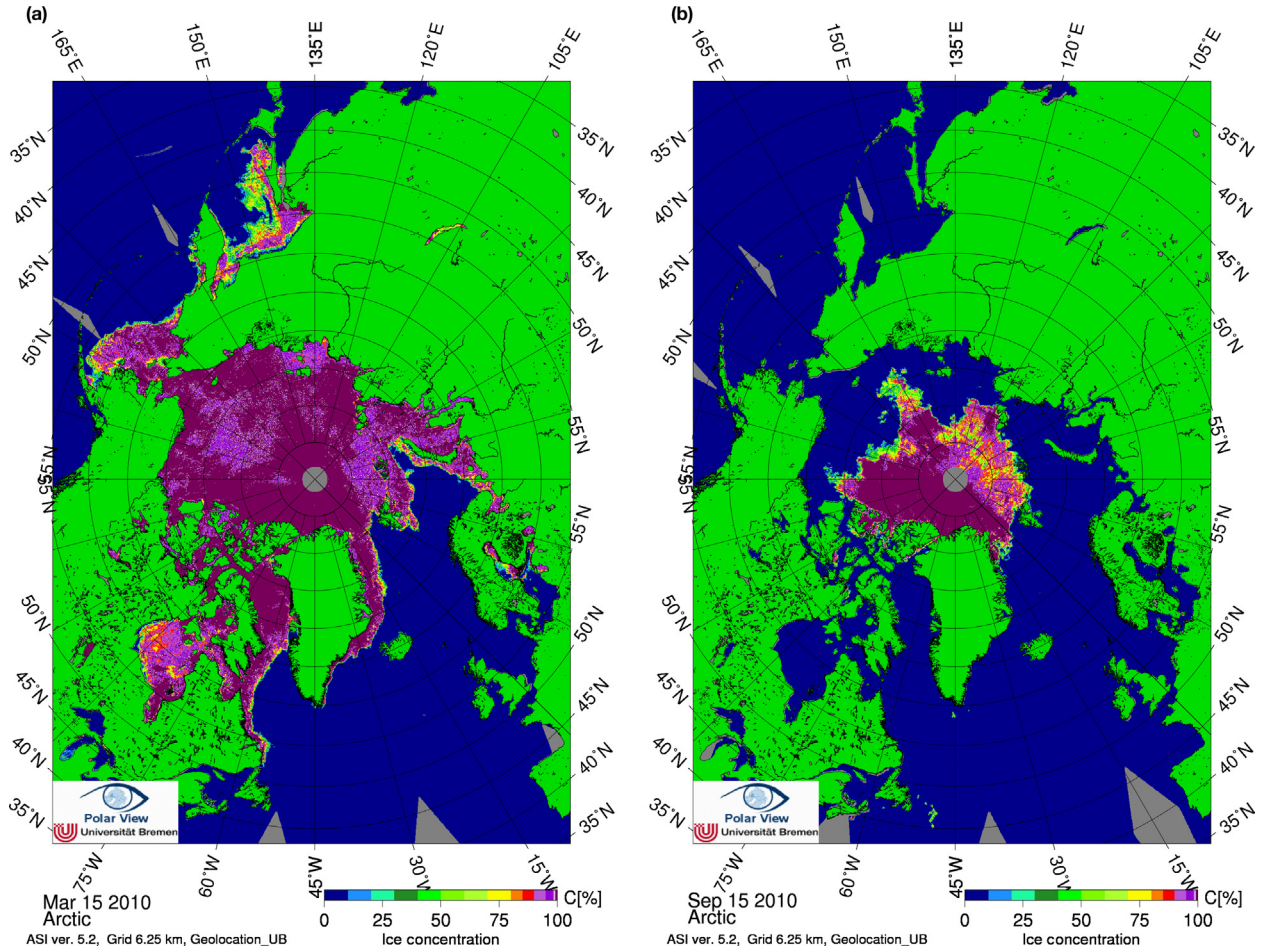

Figure 1 Arctic sea ice concentration for (a) 15 March 2010 and (b) 15 September 2010 based on data from the Advanced Microwave Sounding Radiometer (AMSR-E) aboard the NASA Aqua satellite (University of Bremen, Bremen, Germany).

radiative forcing. The polar vortex is much weaker during summer and is more symmetric than its winter counterpart, with the lowest pressure heights centered roughly over the pole (Figure 3(b)). This shift of the vortex core to over the pole is consistent with the presence of a melting sea ice cover, which strongly inhibits heating of the overlying atmosphere.

The mean annual sea level pressure field (Figure 2) masks large seasonal variability. The dominant sea level features of the mean winter circulation (Figure 4(a)) are the Icelandic Low off the southeast coast of Greenland, the Aleutian Low in the north Pacific basin, and the Siberian High over central Eurasia. In comparison to Figure 2, note the absence of a closed anticyclone over the Beaufort Sea; in winter the region is instead part of a saddle of high pressure extending from the Siberian High across the ocean and into northwestern Canada. The Beaufort Sea high is actually best expressed during spring. The Icelandic and Aleutian Lows are maintained by low-level thermal effects of the comparatively warm and largely ice-free underlying ocean, and position downstream of the major mid-tropospheric stationary troughs where eddy activity is favored. Regional cyclone development processes are also prominent in the vicinity of the Icelandic Low (see Extratropical Cyclone Activity and Polar Lows). The Siberian High is a cold, shallow feature. The Icelandic and Aleutian Lows are much weaker during summer as compared to winter (Figure 4(b)). Summer also sees replacement of the Siberian High by mean low pressure, related in part to strong seasonal heating of the land surface. A weak high-pressure cell is found in the southern Beaufort Sea. An area of mean low pressure is also found centered near the pole.

Extratropical Cyclone Activity and Polar Lows

Winter cyclone activity is most prominent over the Atlantic side of the Arctic (Figure 5(a)). Atlantic-side cyclones typically take a northerly to easterly track and collectively represent part of the North Atlantic cyclone track. Activity peaks in the vicinity of the Icelandic Low. Cyclone development is favored because of temperature contrasts between the warm, northward flowing North Atlantic drift current and the cold, southward flowing East Greenland current, proximity to strong horizontal temperature gradients along the sea ice margin (see Figure 1(a)), and distortions to the atmospheric flow induced by the topography of the Greenland ice sheet. Synoptic events in the vicinity of the

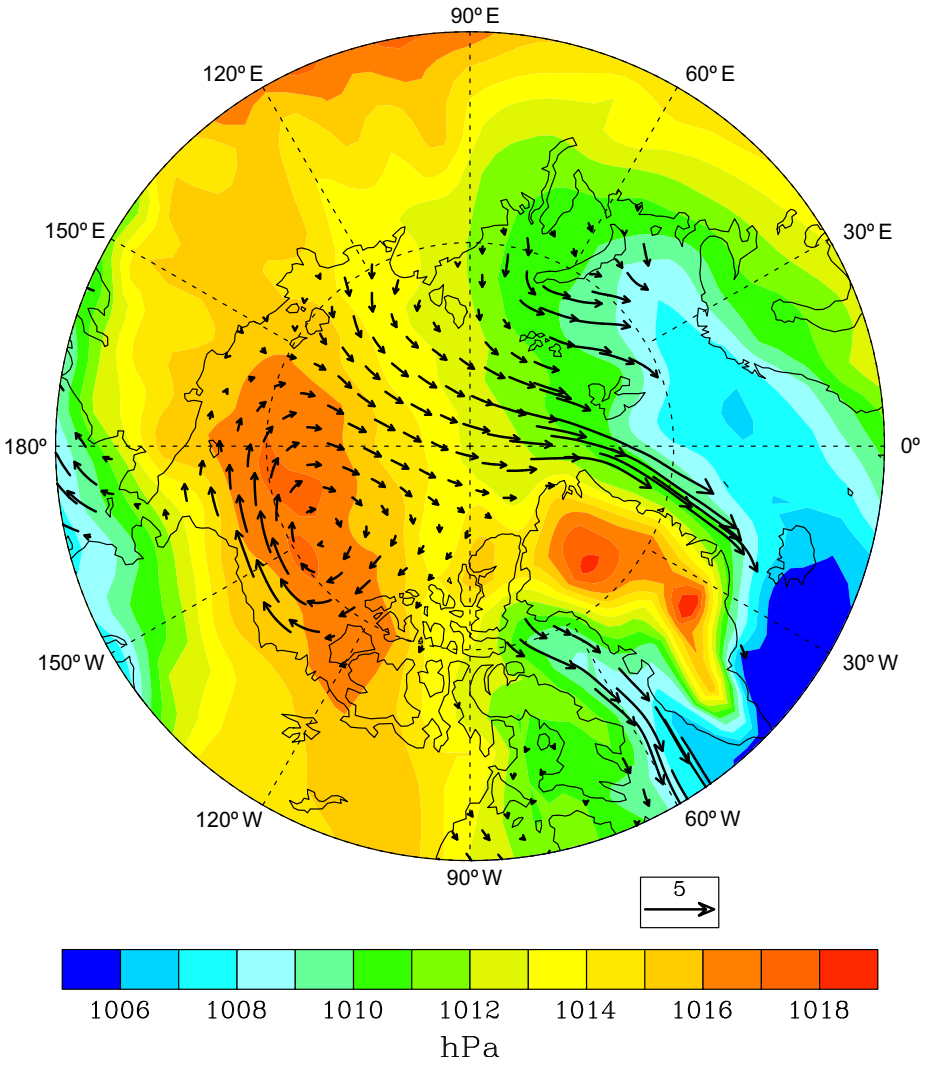

Figure 2 Mean annual sea ice drift (cm s^{-1}), based on data from drifting buoys, manned and unmanned camps and mean annual sea level pressure (hPa, see color scale). Reproduced from Serreze, M.C., Barrett, A.P., 2011. Characteristics of the Beaufort Sea high. Journal of Climate 24, 159–182.

Iceland Low include splitting (bifurcation) of cyclones at the southern tip of Greenland, with one center tracking northward along the west side of Greenland and the other tracking east of Greenland, orographic cyclogenesis in the lee of Greenland, and rapid deepening of existing systems that have migrated into the region from the south.

The North Atlantic cyclone track is weaker in summer, but cyclone activity increases over land (Figure 5(b)). Summer cyclogenesis is favored over northern Eurasia and over Alaska and extending southeast. A summer cyclone maximum is also found over the central Arctic Ocean, centered near the North Pole in the long-term mean. The summer cyclone pattern is associated with the influx of lows generated over the Eurasian continent and cyclogenesis over the Arctic Ocean itself. Systems entering the central Arctic Ocean from the outside, or formed within the region, migrate around the 500 hPa polar vortex, and decay within the cyclone maximum region or in close proximity. These processes help to maintain the weak mean low-pressure cell centered near the pole seen in Figure 4(b).

Polar Lows are cold season mesoscale systems that form within or at the leading edge of polar air streams. Polar Lows are particularly common in the Nordic Seas, the Labrador Sea, the Bering Sea, the Gulf of Alaska, and the Sea of Japan. Polar Lows are typically less than 500 km in diameter. They may intensify rapidly and surface wind speeds can reach hurricane force, but they also tend to be short-lived, existing 3–36 h. When moving over land or the sea ice cover, they tend to rapidly dissipate. They can be thought of as hybrid systems, typically having features of both baroclinic and convective in nature. A common feature of Polar Lows seen in satellite imagery is a spiral cloud (comma cloud) signature. Some systems develop a clear eye at the center similar to tropical cyclones. Rapid intensification of an intense Polar Low seems to require some element of convection. Preferred areas for Polar Low development mentioned above are those that are

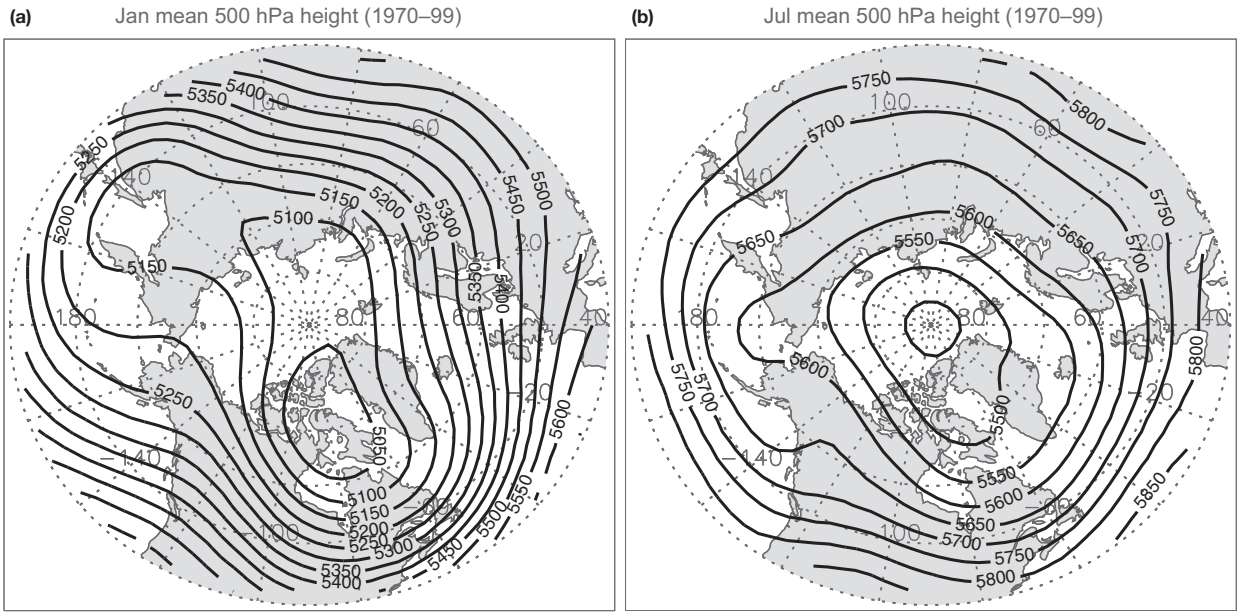

Figure 3 Mean 500 hPa height fields (m) for (a) January and (b) July based on NCEP/NCAR reanalysis data for the period 1970–99.

commonly subject to cold polar outbreaks, where cold continental air is advected over relatively warm open water – conditions favoring convection. This helps explain why Polar Lows are essentially cold season phenomena.

Frontal Activity

The concept of preferred geographical regions of frontal activity in northern high latitudes distinct from frontal activity in middle latitudes (termed the 'Arctic Frontal Zone') has a long history. A maximum in frontal frequencies is found during summer along northern Eurasia from about 60–70° N, best expressed over the eastern half of the continent. A similar relative maximum is found over Alaska, which although best expressed in summer is present year-round. These features are clearly separated from the polar frontal zone in the middle latitudes of the Pacific basin. While some separation between high and middle latitude frontal activity is observed in all

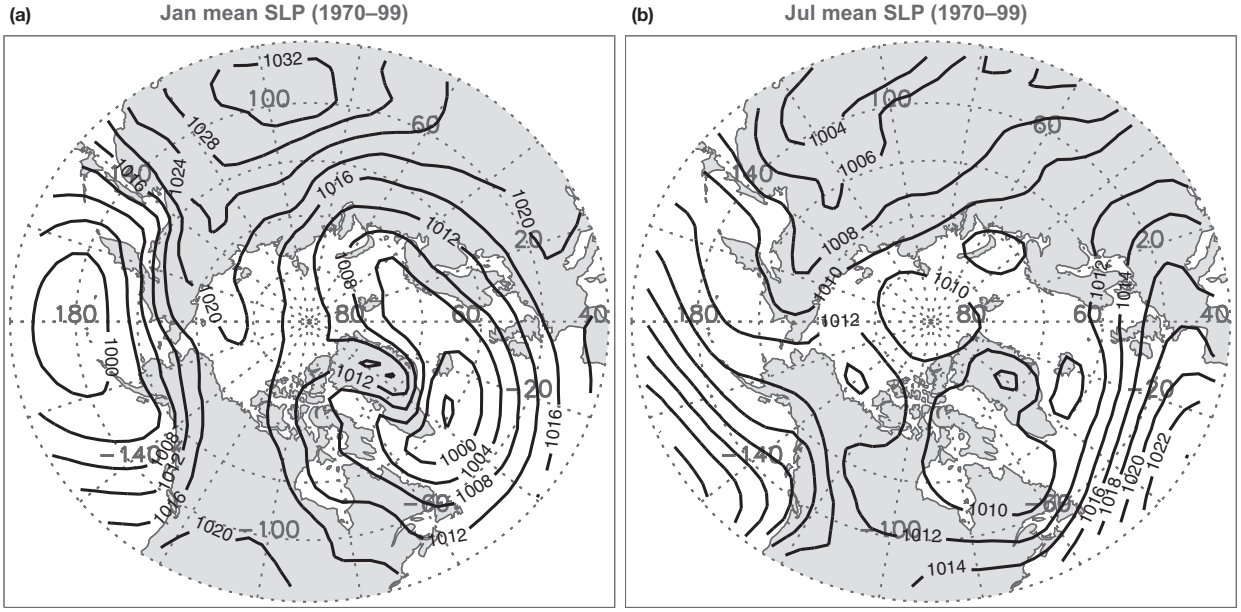

Figure 4 Mean sea level pressure fields (hPa) for (a) January and (b) July based on NCEP/NCAR reanalysis data for the period 1970–99. Note the different contour interval for January (4 hPa) compared to July (2 hPa).

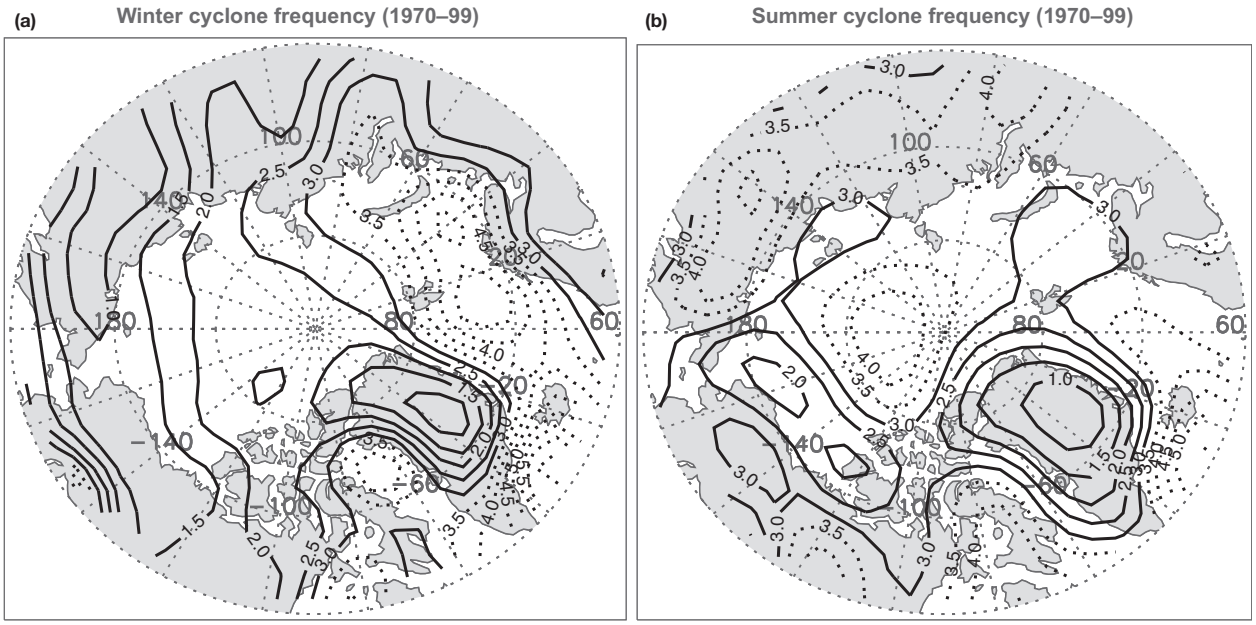

Figure 5 Average seasonal number of extratropical cyclone centers for (a) winter and (b) summer. Results are based on an automated cyclone identification algorithm applied to 6-h sea level pressure fields from the NCEP/NCAR reanalysis for the period 1970–99. Dotted contours are used to highlight areas with more than 3.5 systems per season.

seasons, the summer season is distinguished by the development of a mean baroclinic zone aligned along the Arctic Ocean coastline and associated wind maxima in the upper troposphere. While it has been postulated that the frontal zone arises from contrasts in energy balance between the tundra and boreal forest, it appears that coastal baroclinicity and focusing of the baroclinicity by orography play stronger roles. Regions of maximum summer frontal frequency correspond to preferred areas of summer cyclogenesis over Eurasia and Alaska.

Surface Energy Budget and Cloud Cover

Figure 6 shows typical monthly values of surface radiative flux components for the central Arctic Ocean. The outgoing longwave flux from the surface decreases from about 320 W m^{-2} in summer (when the sea ice surface is melting) to about 200 W m^{-2} in winter. The incoming longwave flux varies between 160 W m^{-2} in winter to 300 W m^{-2} in July. For all months, the net longwave flux is directed away from the surface. The downwelling shortwave (solar) flux is zero during the winter period of polar darkness, rising to about 300 W m^{-2} in June. Because of the high surface albedo (exceeding 0.80 when covered with fresh snow) comparatively little of the solar flux is absorbed by the surface. A fraction of the incoming solar radiation (typically 15%) penetrates into the snow and ice. Net all-wave radiation (net shortwave plus net longwave) is directed away from the surface from October through March and peaks in June at about 80 W m^{-2}. During winter there is a conductive heat flux through the sea ice to the surface. On an annual basis, the sensible and latent heat fluxes together balance 20–50% of the net radiation. During summer, the bulk of the net radiation is used to melt snow and ice. Locally, over areas of open water or thin ice where strong temperature gradients are formed in the boundary layer in winter, upward sensible heat fluxes may reach 600 W m^{-2}. Condensate plumes emanating from wide (>10 km) open water areas (leads) that extend to 4 km in the atmosphere have been observed in winter.

The fundamental difference between the surface energy budgets of the Arctic Ocean, glaciers, and tundra in summer is the portion of net radiation used to melt snow and ice. Once the snow is melted from the tundra, energy can be used in sensible heating of the atmosphere and evaporation (turbulent heat fluxes). The consumption of heat through melt on the ocean and glaciers is about four to six times larger than on the tundra. Consequently, sensible heat is transferred from the atmosphere to the surface of the oceans and glaciers, while it is carried from the surface to the atmosphere in the tundra. Evaporation is, on average, the most significant heat sink on tundra and is considerably larger than on the ocean and glaciers.

A key control on Arctic surface energy budgets is cloud cover. Winter cloud fractions range from 40 to 70%, greatest over the Atlantic side where extratropical cyclone activity is most common. Total cloud fractions rise to 70–90% in summer. There is a rapid increase between April and May, characterized by the development of extensive low-level stratus over the ocean. The seasonality of low-level stratus appears to be strongly controlled by the temperature-dependent formation of atmospheric ice. At temperatures below freezing, the saturation vapor pressure over ice is lower than over liquid water, such that ice particles grow at the expense of supercooled droplets. The concentration of ice crystals is smaller than that of cloud condensation nuclei. Hence a given mass of frozen condensate is distributed among smaller numbers of larger nuclei that grow rapidly to precipitable sizes when the

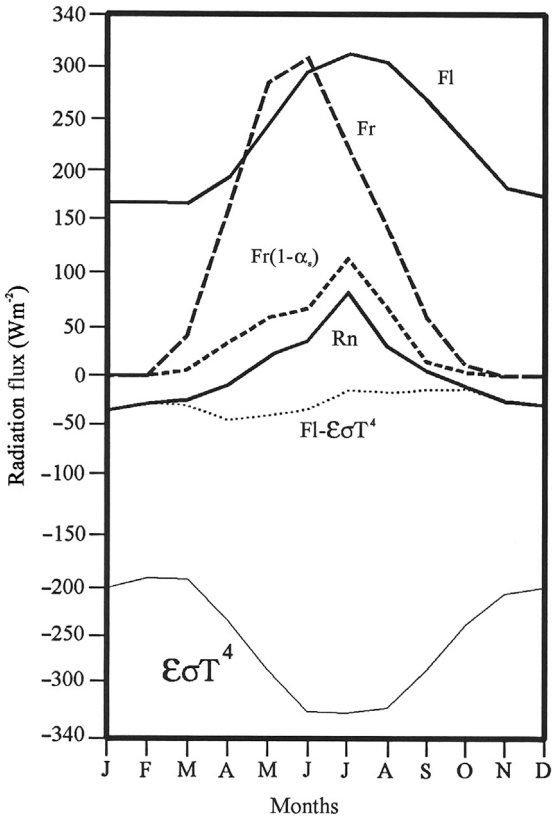

Figure 6 Monthly radiation balance components (W m^{-2}) for the central Arctic Ocean. Notation is as follows: Fl, incoming longwave radiation; Fr, incoming solar radiation; Fr$(1 - \alpha_s)$, solar radiation absorbed at the surface (α_s is surface albedo); Fl $- \varepsilon\sigma T^4$, net longwave radiation; $\varepsilon\sigma T^4$, outgoing (upward) longwave radiation; and Rn, net radiation. Reproduced from Barry, R.G., Serreze, M.C., Maslanik, J.A., Preller, R.H., 1993. The Arctic sea-ice climate system: Observations and modeling. Reviews of Geophysics 31, 397–422.

environment is supersaturated with respect to ice, disfavoring the development of stratus. This can be viewed as a preemptive dissipation of stratus, as the process can prevent the humidity of clear air from reaching saturation. This idea is supported by observations of ice crystal precipitation during the winter months. During summer, when temperatures are higher, the ice crystal scavenging processes are less effective and stratus is more likely to form and persist.

Except for a short period during summer, the net cloud radiative forcing is positive, meaning that clouds have a warming effect at the surface (net radiation at the surface is higher in the presence of clouds). This is basically because the increase in the downwelling longwave radiation flux due to the high emissivity of clouds exceeds the reduction in the downwelling solar radiation flux due to high cloud albedo and to lesser extent cloud absorption. However, cloud radiative forcing is a complex issue, with the sign and magnitude of the forcing depending on the solar flux above the clouds, cloud albedo, optical thickness and temperature, surface albedo, and multiple reflections between the surface and cloud base. Of course during winter, with little or no solar radiation, cloud radiative forcing is always positive.

Air Temperature and Boundary Layer

Winter surface air temperatures decrease sharply from the northern North Atlantic to the central Arctic Ocean (Figure 7(a)). The high temperatures over the Atlantic sector arise from poleward ocean heat transport, which keeps the region free of sea ice, and extensive cloud cover. The lowest winter air temperatures are found over east-central Eurasia in association with the Siberian High. Comparatively higher mean temperatures over the central Arctic Ocean reflect the effect of heat fluxes through areas of open water and thin ice. Low temperatures over the Greenland ice sheet reflect elevation.

Higher summer temperatures over land as compared to the ocean manifest latitude and the transformation of solar radiation into heating the atmosphere from turbulent and upward longwave radiation heat fluxes, as opposed to sea ice melt and seasonal replenishment of the ocean's sensible heat content. These differences in the surface energy budget over land versus ocean (see Surface Energy Budget and Cloud Cover) account for the pronounced temperature gradients along the coast (Figure 7(b)) which are in turn an expression of the summer Arctic frontal zone.

A characteristic feature of the Arctic atmosphere in winter, when there is little or no solar radiation, is a strong surface-based temperature inversion. Away from the Atlantic sector, winter inversions are typically 1000 m deep, with a temperature difference across the inversion layer of 10–12 °C. The winter Arctic inversion can be viewed in terms of an approximate longwave radiative equilibrium. The surface has a longwave emissivity close to one, while the longwave emissivity of the atmosphere is less than one. In longwave equilibrium, the atmosphere must then radiate at a higher physical temperature than the surface, which requires a temperature inversion. However, given that the surface and the atmosphere both radiate to space, maintaining the inversion requires a transport of heat from the south. This provides only a first-order view. Inversion depth and strength vary widely in response to local topographic conditions, winds, cloud cover, and surface fluxes. For example, inversions over the central Arctic Ocean tend to be weaker than over land due to heat fluxes through areas of open water and thin ice. Inversions are also common in summer, although they are weaker than their winter counterparts and are typically separated from the surface by a mixed layer. However, over the Arctic Ocean, shallow surface-based inversions are very common due to sea ice melt, which keeps the surface skin temperature at the melting point, hence leading to the downward sensible heat flux noted earlier.

Hydrologic Budget

Precipitation and Precipitation Minus Evaporation ($P - E$)

Precipitation in the Arctic is difficult to measure accurately because of gauge undercatch of blowing snow, changes in and differences between countries in instrument types and reporting practices, and the sparse precipitation monitoring network. Figure 8 shows the distribution of annual precipitation based on a gridded climatology compiled from several data sources. The highest totals are found off the southeast coast of Greenland (locally >2400 mm) with amounts decreasing

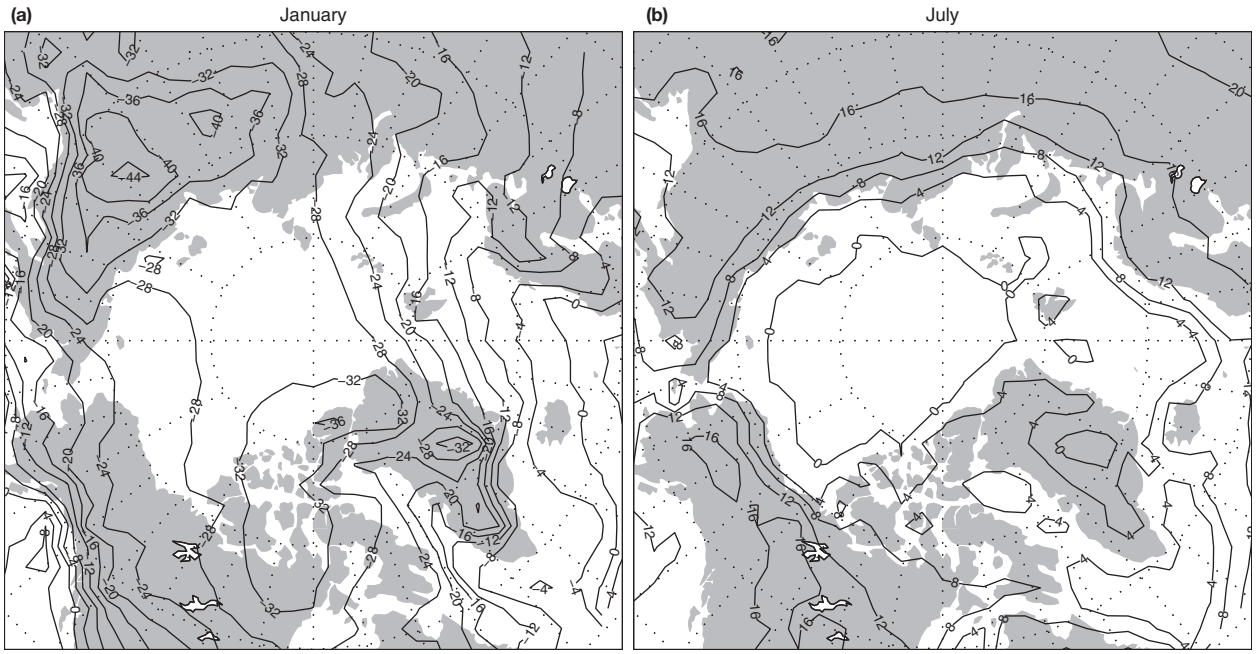

Figure 7 Mean surface air temperature (°C) for (a) January and (b) July, based on the University of Washington International Arctic Buoy Programme/Polar Exchange at the Sea Surface (IABP/POLES) data set. Reproduced from Rigor, I.G., Colony, R.L., Martin, S., 2000. Variations in surface air temperature observations in the Arctic, 1979–1997. Journal of Climate 13, 896–914.

northeast to about 400 mm in the Kara Sea. This pattern manifests the pattern of cyclone activity shown in Figure 5(a). High totals are also found over southern Alaska. The lowest annual totals (<200 mm) encompass the Beaufort Sea and the Canadian Arctic Archipelago; these islands are primarily classified as polar desert. The winter pattern is qualitatively similar to that seen in the annual mean. For example, mean January precipitation ranges from over 200 mm in the northern North Atlantic to less than 10 mm over northern Canada and east-central Eurasia. Summer precipitation is more uniform across the Arctic with markedly higher totals as compared to winter over land areas. This is consistent with seasonal changes in synoptic activity (compare Figure 5(a) and 5(b)). Convective precipitation is not uncommon over Arctic land areas during summer.

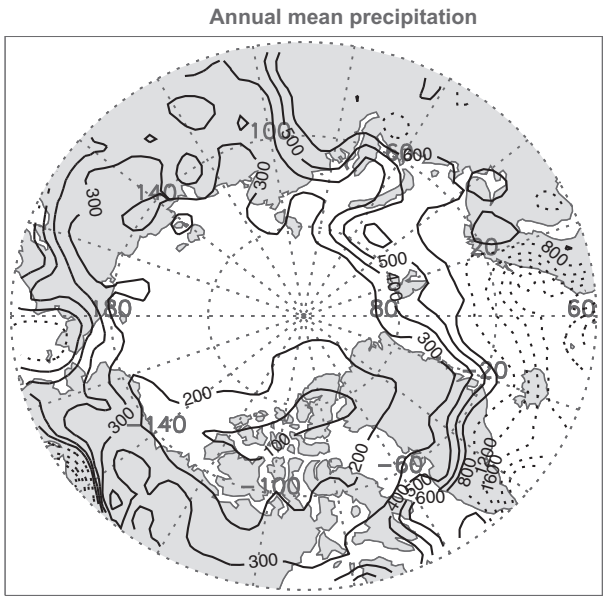

Figure 8 Mean annual precipitation (mm) with estimated adjustments for wind-induced gauge undercatch, changes in instrument types and differences in observing methods. Dotted contours are used to highlight areas with precipitation exceeding 800 mm. Compiled from data provided by Groisman, P., Yang, D., Eischeid, Willmott, C.

Winter precipitation is largely stored in the snowpack. Maximum spring snow depths are highly variable due to differences in precipitation, temperature, topographic setting, and redistribution by wind. Values of 20–50 cm over the Arctic Ocean and 40–70 cm over the subarctic can be considered typical. Mean hydrographs for Arctic rivers exhibit a late spring to early summer peak in discharge due to melt of the snowpack.

Direct estimates of evaporation are scanty. However, large-scale estimates of precipitation minus evaporation ($P - E$) (net precipitation) can be obtained through evaluation of the atmospheric vapor flux convergence. Estimated mean annual $P - E$ (Figure 9) is typically 150–300 mm over land, 200 mm over the central Arctic Ocean and over 1000 mm in the vicinity of the Icelandic Low. Although precipitation over much of the land area peaks in summer, $P - E$ for this season (not shown) tends to be small or even negative. Negative values imply net drying.

Freshwater Budget

The freshwater balance of the Arctic Ocean is a topic of continuing interest. Freshwater storages and transports have typically been calculated with respect to a reference salinity of 34.8 parts per thousand, which approximates the average bulk salinity of the Arctic Ocean. Water lower than this reference

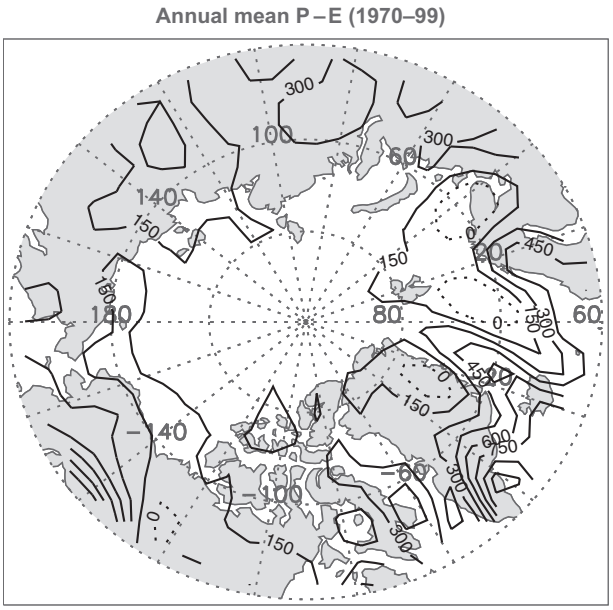

Figure 9 Mean annual precipitation minus evaporation ($P - E$) (in mm) based on calculations of the vapor flux convergence using NCEP/NCAR reanalysis data for the period 1970–99. Areas with negative $P - E$ are indicated with dotted contours.

salinity is said to contain freshwater; the lower the salinity, the greater the freshwater content per unit volume.

The total annual freshwater input to the Arctic Ocean is estimated at about 8500 km^3. The primary inputs are river runoff (38%), the import of fairly low-salinity water through Bering Strait (30%) and positive $P - E$ over the Arctic Ocean itself (24%). The Arctic Ocean is unique in receiving runoff from four of the world's major rivers (the Ob, Yenisei, and Lena in Eurasia and the Mackenzie in North America). These riverine, atmospheric, and oceanic freshwater sources collectively help to maintain a fairly fresh surface layer that extends down to about 200 m, which is often well-mixed down to about 50 m. Relatively warm and salty waters of Atlantic origin are found between 200 and 900 m depth, which if brought to the surface would quickly melt the sea ice cover. However, at low water temperatures of the Arctic Ocean, the density structure is determined by salinity. Hence the fresh surface layer suppresses vertical mixing with the Atlantic layer, and allows sea ice to form readily in winter.

Freshwater export out of the Arctic Ocean and into the North Atlantic is primarily via Fram Strait in the form of low-salinity sea ice (25%) and liquid water (26%), and through the channels of the Canadian Arctic Archipelago, primarily in liquid form (25%). Freshwater export through Fram Strait in particular is believed to impact on the overturning cell of the global ocean through influencing convection in the subarctic gyres which in turn feed the North Atlantic.

Mean annual freshwater input to the Arctic Ocean is roughly an order of magnitude less than the mean freshwater storage in the Arctic Ocean of about 84 000 km^3. This storage is represented by both sea ice and fairly low salinity near surface waters. Assuming steady state, the relative magnitudes of the mean storage versus total inputs (or outputs) imply a mean residence time of freshwater in the Arctic Ocean of about a decade.

Variability and Change in Arctic Climate

Arctic climate exhibits pronounced variability on interannual to decadal scales. A major source of variability is associated with the phase of the North Atlantic Oscillation (NAO), which describes mutual strengthening and weakening of the Azores High and the Icelandic Low. Under the positive mode of the NAO (a deep Icelandic Low), positive temperature anomalies are found over the Eurasian Arctic with negative anomalies over northeastern Canada and the northern North Atlantic. In turn, the North Atlantic cyclone track extends deeper into the Arctic Ocean. Broadly opposing anomalies are associated with negative NAO states. The NAO can be viewed as the North Atlantic component of the Arctic Oscillation (AO) (also called the Northern Annular Mode (NAM)). The AO represents the leading empirical orthogonal function of monthly sea level pressure anomalies poleward of 20° N. Pressure variability associated with the AO is characterized by a primary center of action over the Arctic Ocean, strongest in the vicinity of the Icelandic Low, and opposing anomalies in midlatitudes of the Pacific and Atlantic basins. Changes in the AO index hence manifest a transfer of atmospheric mass between the Arctic and middle latitudes. Time series of the AO and NAO are highly correlated. Arctic climate variability is also linked to the El-Niño Southern Oscillation (ENSO), particularly as it relates to variability in the strength and location of the Aleutian Low, the Pacific North American (PNA) teleconnection, and other modes of variability such as the North Pacific Oscillation (NPO).

The period from the 1970s onward has seen pronounced change in the northern high-latitude environment. Increases in surface air temperature encompass all seasons but are strongest in autumn and winter, and are larger than increases observed for the globe as a whole. Paleoclimate evidence suggests that Arctic temperatures of the late twentieth century and onward are the highest of at least the past 2000 years. Analysis of satellite data available since 1979 documents negative linear trends in sea ice extent for all months, with the strongest trend in September, the end of the summer melt season (13% per decade over 1979–2012 relative to 1979–2000 mean; see http://nsidc.org/) (Figure 10). A key driver of this seasonal asymmetry in trends is that the spring ice cover is increasing dominated by relatively thin first-year ice, with less of the generally thicker multiyear ice. As it takes less energy to melt out thin ice, the thinner the ice in spring, the lower the ice extent at the end of summer. Thin spring ice also fosters earlier exposure of dark open water areas in summer which strongly absorb solar energy, leading to a warming ocean that fosters more melt. Other changes include increased vegetation growth, with areas of tundra replaced by shrub vegetation, warming and thawing of permafrost, increased discharge of Arctic-draining rivers in Eurasia, and increased coastal erosion due to a combination of sea ice retreat that allows for stronger wave action, and a warming ocean.

Climate models project that the effects of rising concentrations of atmospheric greenhouse gases will be especially

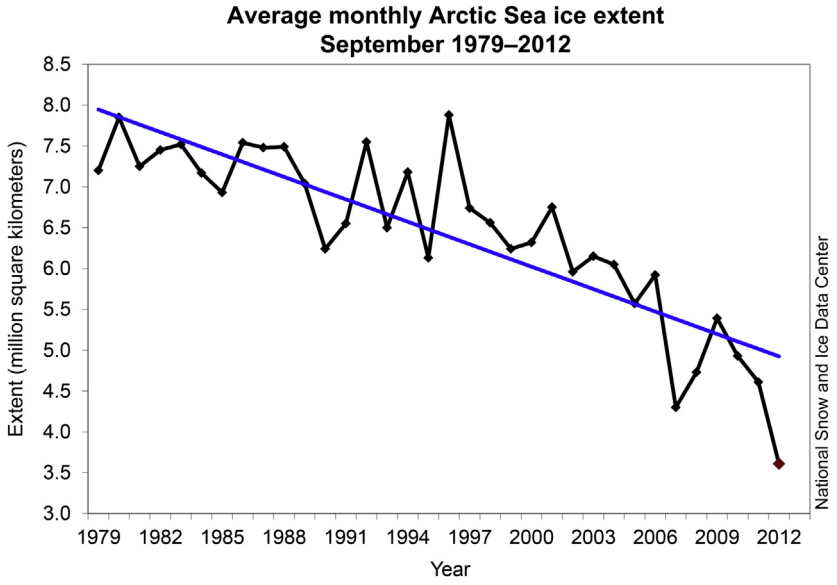

Figure 10 September sea ice extent, 1979–2012, with linear least squares fit (blow line), based on analysis of satellite passive microwave data distributed by the National Snow and Ice Data Center, Boulder, Colorado.

strong in the Arctic due to feedbacks in which variations in sea ice and snow extent, the stability of the lower troposphere, and thawing of permafrost play key roles. However, regional patterns of Arctic warming differ greatly among simulations. Projected warming is generally strongest for autumn and winter, largely because of the delayed growth of sea ice, which allows for large fluxes of heat from the ocean to the atmosphere. Retreat of snow cover and sea ice is accompanied by increased winter precipitation. Observed changes in the Arctic environment over the past decade are generally viewed as reflecting the combined influences of natural variability in patterns of atmospheric and oceanic circulation having strong regional expressions, superposed upon a general warming linked to fossil fuel burning.

See also: **Cryosphere:** Permafrost; Sea Ice; Snow (Surface). **Climate and Climate Change:** Climate Variability: North Atlantic and Arctic Oscillation. **Global Change:** Climate Record: Surface Temperature Trends. **Middle Atmosphere:** Polar Vortex. **Radiation Transfer in the Atmosphere:** Cloud-Radiative Processes. **Synoptic Meteorology:** Extratropical Cyclones; Fronts; Polar Lows.

Further Reading

ACIA, 2005. Impacts of a Warming Arctic: Arctic Climate Impact Assessment. Cambridge University Press, Cambridge, UK.

Beesley, J.A., Moritz, R.E., 1999. Toward an explanation of the annual cycle of cloudiness over the Arctic Ocean. Journal of Climate 12, 395–415.

Bekryaev, R.V., Polyakov, I.V., Alexeev, V.A., 2010. Role of polar amplification in long-term surface air temperature variations and modern arctic warming. Journal of Climate 23, 3888–3906.

Cullather, R.I., Bromwich, D.H., Serreze, M.C., 2000. The atmospheric hydrologic cycle over the Arctic basin from reanalyses. Part I: Comparison with observations and previous studies. Journal of Climate 13, 923–937.

Curry, J.A., Rossow, W.B., Randall, D., Schramm, J.L., 1996. Overview of Arctic cloud and radiation characteristics. Journal of Climate 9, 1731–1764.

Dimitrenko, I.A., Polyakov, I.V., Krillov, S.A., et al., 2008. Toward a warmer Arctic Ocean: Spreading the early 21st century Atlantic Water warm anomaly along the Eurasian Basin margins. Journal of Geophysical Research 113, C05023. http://dx.doi.org/10.1029/2007JC004158.

Kaufman, D.S., Schneider, D.P., McKay, N.P., et al., 2009. Recent warming reverses long-term Arctic cooling. Science 325, 1–4.

National Snow and Ice Data Center http://nsidc.org/ [accessed 23.03.12].

Ohmura, A., 1984. Comparative energy balance study for Arctic tundra, sea surface, glaciers and boreal forests. GeoJournal 8, 221–228.

Renfrew, I.A., 2003. Polar Lows. In: Holton, J.R., Curry, J.A., Pyle, J.A. (Eds.), Encyclopedia of Atmospheric Sciences. Academic Press, London, UK/San Diego, CA, pp. 1761–1768.

Screen, J.A., Simmonds, I., 2010. The central role of diminishing sea ice in recent Arctic temperature amplification. Nature 464, 1334–1337.

Serreze, M.C., Barrett, A.P., Slater, A.G., et al., 2006. The large-scale freshwater cycle of the Arctic. Journal of Geophysical Research 110, C11010. http://dx.doi.org/10.1029/2005JC003424.

Serreze, M.C., Barry, R.G., 2005. The Arctic Climate System. Cambridge University Press, Cambridge, UK.

Serreze, M.C., Lynch, A.H., Clark, M.P., 2001. The Arctic frontal zone as seen in the NCEP/NCAR reanalysis. Journal of Climate 14, 1550–1567.

Stroeve, J., Serreze, M., Drobot, S., et al., 2008. Arctic sea ice extent plummets in 2007. EOS. Transactions, American Geophysical Union 89, 13–14.

Thompson, D.W.J., Wallace, J.M., 2001. Regional climate impacts of the Northern Hemisphere Annular Mode. Science 293, 85–89.